Split-pulse spectrometer for absolute XUV frequency measurements

I. Liontos,[1,*] C. Corsi,[1] S. Cavalieri,[1,2] M. Bellini,[1,3] and R. Eramo[1,3]

[1]*European Laboratory for non linear Spectroscopy (LENS), 50019 Sesto Fiorentino, Florence, Italy*

[2]*Department of Physics, University of Florence, 50019 Sesto Fiorentino, Florence, Italy*

[3]*Istituto Nazionale di Ottica (INO-CNR), Largo Enrico Fermi 6, 50125 Florence, Italy*

**Corresponding author: liontos@lens.unifi.it.*

Received February 2, 2011; revised April 22, 2011; accepted April 26, 2011;
posted April 28, 2011 (Doc. ID 141930); published May 26, 2011

A split-pulse spectrometer based on pairs of time-delayed femtosecond pulses can give access to accurate frequency measurements in the extreme ultraviolet (XUV) spectral domain. We demonstrate this approach by measuring the absolute frequency of a single-XUV-photon transition to a bound state of atomic argon excited with the ninth harmonic of an amplified Ti:sapphire laser. © 2011 Optical Society of America

OCIS codes: 300.6540, 300.6320, 300.6300, 190.4160.

Extending high-resolution spectroscopy to the vacuum and extreme ultraviolet (VUV and XUV) regime is highly desirable, because in this spectral region lie many atomic transitions that would allow accurate testing of bound-state quantum electrodynamics [1]. So far, the main sources of broadband radiation in the XUV are provided by synchrotron facilities that, when used in combination with the best monochromators, lead to a spectral resolution of about 0.5–1.0 cm^{-1} [2], corresponding to a resolving power around 10^5. On the other hand, high-order harmonic (HOH) generation from intense femtosecond laser pulses, with its tabletop character, is an effective and attractive alternative tool for producing coherent radiation in this spectral region. The main limitation of its application to high-resolution spectroscopic studies, its inherently broad bandwidth, has been overcome by utilizing time-delayed pulse replicas to excite the targeted atomic system, in analogy to the Ramsey scheme of separated oscillatory fields [3]. For the simplest system (two levels with transition frequency ν_{eg} and lifetime $\tau \gg t$, t being the delay between the pulses, assuming vacuum propagation), the excited-state population at the end of the second pulse (of central frequency ν) is given, at the first order of a perturbative expansion [4,5], by

$$|c_e(t)|^2 = \frac{|\tilde{\Omega}(\nu - \nu_{\mathrm{eg}})|^2}{4} |1 + e^{2\pi i \nu_{\mathrm{eg}} t}|^2, \qquad (1)$$

where the amplitude factor, which coincides with the single-pulse excitation, is the squared modulus of the Fourier transform (FT) of the (single-pulse) Rabi frequency Ω. Thus, the excitation appears periodically modulated at the transition frequency ν_{eg}.

Two different experimental methods have been adopted so far to apply Ramsey's idea in the temporal domain for VUV and XUV spectroscopy: one approach selects and amplifies to the millijoule level a pair of subsequent pulses from an IR frequency comb (FC) laser [6–8]; the other approach, which will be followed here, creates the required pulse pair by splitting an amplified mode-locked IR laser pulse in a Michelson interferometer [9–11]. In both cases, the IR pulse-pair is frequency upconverted to the XUV via HOH generation in a gas medium and is then used for excitation of the atomic energy levels under investigation. An important advantage of the FC approach is that the pulse-pair time delay is directly given by the inverse of the FC frequency repetition rate; yet, at the same time, its applicability is intrinsically limited to the excitation of states whose lifetimes are longer than the FC interpulse delay, currently around 10 ns. The split-pulse technique [5] successfully demonstrated in autoionizing [9,10,12] and bound states [11], does not suffer this limit. However, to our knowledge, it has never been employed for absolute frequency measurements.

In principle, and similarly to FT methods, obtaining absolute frequency determinations in a complex spectrum or simply gaining information on the broadening processes present in the case of the single oscillator [Eq. (1)], would imply the measurement of Ramsey fringes over the complete time-delay range $[0, T]$, $1/T$ being fixed by the resolution goal. However, considering that the fringes to be recorded in the XUV have a period in the attosecond time scale, such measurements (performed in a slow ion/electron count regime) are easily seen to require prohibitively long acquisition times. As a matter of fact, the current stability-related constraints dictate maximum scan times of the order of $\delta t \approx 10$ fs, which imply a frequency resolution $(1/\delta t)$ of thousands of wavenumbers. Nonetheless, if the investigated spectrum is made of only a single narrow line, then things are much simpler and the $1/\delta t$ limit can easily be beaten. In fact, by just measuring the phase of the oscillating fringes and knowing the origin $t = 0$, a measurement can be made with a δt scan around T, leading to a frequency determination with an accuracy $\approx 1/T$. There is an inherent ambiguity in this procedure, as both ν_0 and $\nu_0 + \Delta\nu$ will lead to the same fringe phase, provided that $T\Delta\nu$ is an integer; in other words, the observed fringe determines the resonance frequency modulo $1/T$. This ambiguity can be resolved if a previous measurement exists with an accuracy much better than $1/T$, or by combining the results of measurements made at properly chosen delays [13]. In the FC-based Ramsey technique, the zero-time-delay position between the pulse pair is precisely known with an error that is small with respect to the transition wavelength to be measured

(also when this lies in the XUV range). In our split-pulse case, determining the $t = 0$ position is also possible by finding the symmetry point of the IR linear interferometric autocorrelation signal in the Michelson interferometer, but a different, specifically devised, approach has been developed in this work. Here we perform measurements of pairs of δt scans whose starting times have a relative delay T, which is also measured with sub-XUV-wavelength accuracy. In addition, this procedure leads to a comparison between the phases of the two measurements, and thus to an absolute measurement of ν_{eg}.

The relevant atomic levels and the ionization pathway, as well as the experimental setup, are schematically shown in Fig. 1. A single-photon-XUV transition at 87 nm in atomic argon is investigated. The XUV pulse pair excites the $3s^2 3p^5 (^2P_{1/2}) 3d$ level, which lies at $\nu_{eg} = 115366.87\ \mathrm{cm}^{-1}$ above the ground state [14], while photoionization is achieved by a single-IR-photon absorption at the fundamental wavelength. A more detailed description of the setup can be found in [10,11]. In brief, the light source is provided by an amplified Ti:sapphire laser (up to 0.8 mJ energy per pulse, 25 fs pulse duration, 1 kHz repetition rate, central wavelength set at 794 nm). The main part of the laser emission is sent to a semimonolithic Michelson interferometer, which splits the incoming pulse, creating the pairs. The IR beam is then focused into a vacuum chamber where it interacts with a continuous-flow xenon gas jet. The different harmonic orders generated are dispersed by a concave normal-incidence grating, and the ninth harmonic (87 nm), nearly resonant with the atomic transition, is refocused onto a second jet of argon atoms in the interaction chamber. The time-delayed (1 ns) IR ionizing beam is obtained by intercepting a fraction of the fundamental laser emission and focusing it onto the excited argon atoms in a counterpropagating direction with respect to the XUV pulse pair. Finally, the Ar ions are detected by a time-of-flight (TOF) mass spectrometer [11]. The moving mirror of the Michelson interferometer is mounted on a motorized stage that moves in steps of ≈3.5 nm. Sub-XUV-wavelength accuracy in the measurement of the Michelson path displacement is accomplished by a continuous recording of the interference fringes of two collinear and in-quadrature polarizations from a He–Ne laser of known frequency (at the GHz level). The two linear polarizations are obtained by using a $\lambda/8$ waveplate in one arm of the interferometer; they are separated at the exit of the interferometer by a beam-splitter cube and then sent to two photodiodes (PDs). The temperature and pressure dependence of the air-refractive index in the beam path has been taken into account for this wavelength-based determination of the delay.

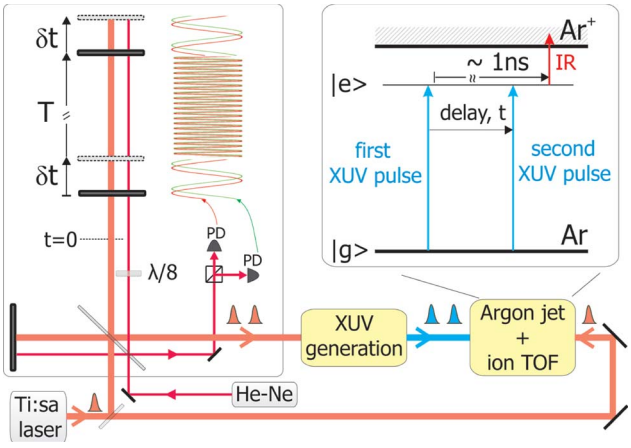

Fig. 1. (Color online) Scheme of the experimental setup. Left inset: Michelson interferometer and scheme of the two-time-window measurement. Right inset: relevant Ar levels and pulse sequences.

Measurements are performed in three consecutive stages, also schematically depicted in Fig. 1: first, the Ar^+ Ramsey fringes are recorded over a short- (and slow-) delay time window δt of about 5–10 fs, beginning from an initial delay of 100 fs away from the $t = 0$ position to avoid intensity-related interference effects. Then, the delay is rapidly swept for the measurement delay T and, finally, another short and slow fringe scan of δt duration is performed. A typical two-time-window acquisition is presented in Fig. 2. Figures 2(a) and 2(b) show the δt scans, where the ionization events exhibit Ramsey oscillations of good visibility. In Figs. 2(c) and 2(d) we report the corresponding interference signal of the two in-quadrature He–Ne beams. In Fig. 2(g), we present a zoom of the squared modulus of the FT of the pair around the theoretical value of the transition frequency under study [14]. As expected, the modulation has a period of $1/T$, i.e., it shows a mode structure whose peak frequencies can be denoted as $\nu_m(T)$, where $m = 0, \pm 1, \pm 2, \cdots$ labels the modes starting from the one nearest the NIST frequency ν_{NIST}. In Figs. 2(e) and 2(f), the two spectra corresponding to the separate single scans are also plotted. These two spectra show the broad sinc^2-shaped form related to the sampling time window δt. The analysis of the He–Ne fringes for this particular

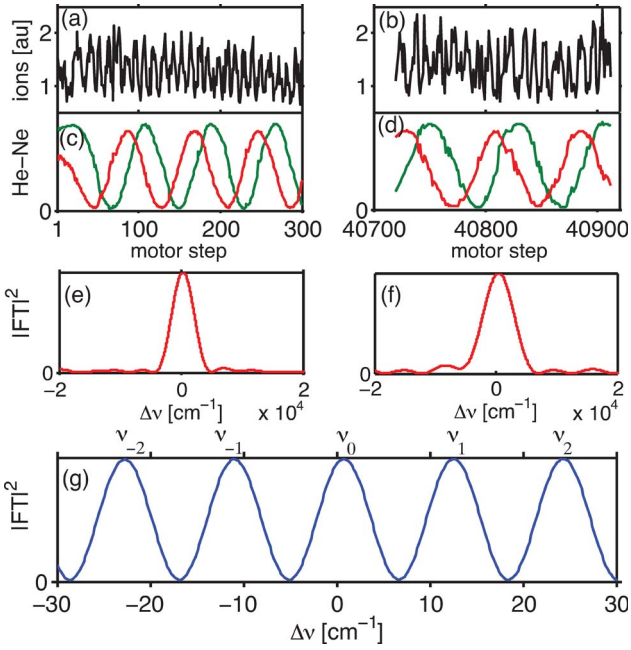

Fig. 2. (Color online) (a), (b) Ramsey fringes for two slow and short scans delayed by $T \approx 2.84$ ps; (c), (d) corresponding He–Ne interference fringes; (e), (f) squared FT of the above fringe patterns; (g) spectrum of the combined two-time-window acquisition; modes labels $\nu_o, \nu_{\pm 1}, \ldots$ are also indicated. The origin of the frequency is ν_{NIST}.

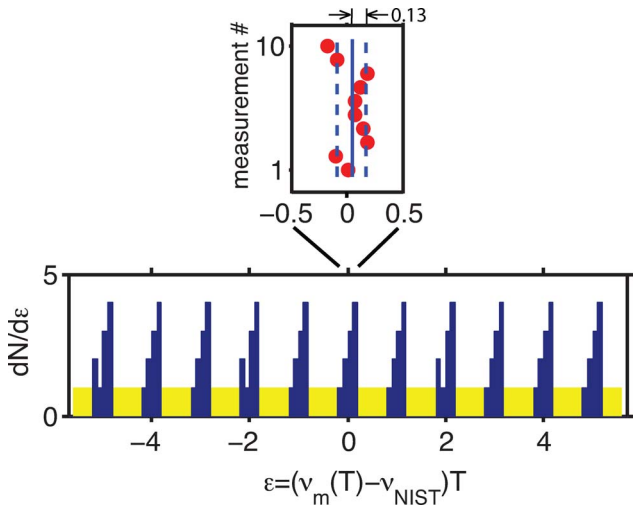

Fig. 3. (Color online) Histogram of the mode frequencies $\nu_m(T)$ versus the adimensional variable $\epsilon = T(\nu_m(T) - \nu_{\mathrm{NIST}})$. The peaks have a standard deviation of 0.13. For comparison, a completely flat distribution due to large calibration errors (the band drawn on the bottom of the histogram) would be characterized by a standard deviation ≈0.29.

measurement leads to a Michelson mirror displacement $L = 425154\,\mathrm{nm}$ between the beginnings of the two δt scans, corresponding to a delay, $T = 2L/v_g \approx 2.84\,\mathrm{ps}$ (v_g is the group velocity in air at the IR fundamental frequency ν_{IR}), and to a Ramsey modulation frequency of $1/T \approx 11.8\,\mathrm{cm}^{-1}$. In this case, the center of the high-frequency modulation is detuned $0.8\,\mathrm{cm}^{-1}$ from the NIST reference, i.e., 7% of the fringe period, implying a systematic error on the determination of the mirror movement of $0.07 \cdot \lambda_{\mathrm{xuv}}/2 \approx 3\,\mathrm{nm}$ [15]. As a check of the validity of our approach, in Fig. 3 we plot the offset $\nu_m - \nu_{\mathrm{NIST}}$ of the mode frequencies normalized to the mode separation $1/T$ for ten different measurements in the range $T = 0.9$–$4.2\,\mathrm{ps}$. The frequencies are collected around integer values; the width of these peaks, dominated by the error on the delay T, is fully compatible with the expected positioning error, $\Delta L \approx 5\,\mathrm{nm}$, of the Michelson arms as independently deduced from a comparative analysis of the two in-quadrature He–Ne fringes. It is important to stress that, as ΔL is roughly independent on L, the accuracy of the measurement can be improved by using longer delays. The clear evidence of a mode structure in Fig. 3 is a signature that our setup is indeed measuring the XUV atomic frequency. We can summarize our results by reporting the mean frequency shift $\langle \nu_0 - \nu_{\mathrm{NIST}} \rangle = (0.4 \pm 1.4)\,\mathrm{cm}^{-1}$.

In conclusion, we have demonstrated the potential of the split-pulse approach in the determination of a transition frequency of atomic argon. By using pairs of Ramsey-like measurements, following the ionization signal in two temporal windows whose starting times are accurately measured through the fringes of a reference laser, we obtain an absolute measurement of an XUV transition with an accuracy of a few parts in 10^5. The presented idea has the potential to aim at higher resolutions and appears to be the only viable approach that provides and alternative to synchrotron radiation for unstable (e.g., autoionizing) states, when the lifetime gets below the current limit of FC sources.

This work was partially supported by Ente Cassa di Risparmio di Firenze, by the European Commission (EC)'s Seventh Framework Programme (FP7) under grant agreement n.228334 (JRA1: ALADIN), and by Regione Toscana under project CTOTUS. We acknowledge R. Ballerini, A. Hajeb, M. Giuntini, M. De Pas, and A. Montori for technical assistance.

References and Notes

1. M. Herrmann, M. Haas, U. D. Jentschura, F. Kottmann, D. Leibfried, G. Saathoff, C. Gohle, A. Ozawa, V. Batteiger, S. Knünz, N. Kolachevsky, H. A. Schüssler, T. W. Hänsch, and T. Udem, Phys. Rev. A **79**, 052505 (2009).
2. P. A. Heimann, M. Koike, C. W. Hsu, D. Blank, X. M. Yang, A. G. Suits, Y. T. Lee, M. Evans, C. Y. Ng, C. Flaim, and H. A. Padmore, Rev. Sci. Instrum. **68**, 1945 (1997).
3. N. Ramsey, Phys. Rev. **78**, 695 (1950).
4. M. M. Salour, Rev. Mod. Phys. **50**, 667 (1978).
5. S. Cavalieri and R. Eramo, Phys. Rev. A **58**, R4263 (1998).
6. S. Witte, R. T. Zinkstok, W. Ubachs, W. Hogervorst, and K. S. E. Eikema, Science **307**, 400 (2005).
7. R. T. Zinkstok, S. Witte, W. Ubachs, W. Hogervorst, and K. S. E. Eikema, Phys. Rev. A **73**, 061801 (2006).
8. D. Z. Kandula, C. Gohle, T. J. Pinkert, W. Ubachs, and K. S. E. Eikema, Phys. Rev. Lett. **105**, 063001 (2010).
9. S. Cavalieri, R. Eramo, M. Materazzi, C. Corsi, and M. Bellini, Phys. Rev. Lett. **89**, 133002 (2002).
10. A. Pirri, E. Sali, C. Corsi, M. Bellini, S. Cavalieri, and R. Eramo, Phys. Rev. A **78**, 043410 (2008).
11. I. Liontos, S. Cavalieri, C. Corsi, R. Eramo, S. Kaziannis, A. Pirri, E. Sali, and M. Bellini, Opt. Lett. **35**, 832 (2010).
12. E. Skantzakis, P. Tzallas, J. E. Kruse, C. Kalpouzos, O. Faucher, G. D. Tsakiris, and D. Charalambidis, Phys. Rev. Lett. **105**, 043902 (2010).
13. R. Eramo, M. Bellini, C. Corsi, I. Liontos, and S. Cavalieri, Phys. Rev. A **83**, 041402 (2011).
14. Y. Ralchenko, A. E. Kramida, J. Reader and NIST Atomic Spectra Database (ASD) Team, "NIST Atomic Spectra Database (version 4.0.1)" (National Institute of Standards and Technology, 2010), available online at: http://physics.nist.gov/asd.
15. Note that the frequency origin of our plots takes into account the carrier envelope offset correction, whose effect is to decrease the apparent frequency of the transition in Eq. (1): $\nu_{\mathrm{eg}} \to \nu_{\mathrm{eg}} - \delta\nu_{\mathrm{ceo}}$, $\delta\nu_{\mathrm{ceo}} = N_h \nu_{\mathrm{IR}}(1 - n v_g/c) = +0.56\,\mathrm{cm}^{-1}$, where $N_h = 9$ is the order of the harmonic, while n is the refractive index at ν_{IR}.